



A procedure to select ground-motion time histories for deterministic seismic hazard analysis from the Next Generation Attenuation (NGA) database

Duruo Huang¹, Wenqi Du², and Hong Zhu³

¹Department of Civil and Environmental Engineering and Institute for Advanced Study, Hong Kong University of Science and Technology, Kowloon, Hong Kong SAR, China

²Institute of Catastrophe Risk Management, Nanyang Technological University, Singapore

³Department of Civil and Environmental Engineering, Hong Kong University of Science and Technology, Kowloon, Hong Kong SAR, China

Correspondence to: Duruo Huang (huangdr@ust.hk)

Received: 22 January 2017 – Discussion started: 20 February 2017

Revised: 11 August 2017 – Accepted: 29 August 2017 – Published: 6 October 2017

Abstract. In performance-based seismic design, ground-motion time histories are needed for analyzing dynamic responses of nonlinear structural systems. However, the number of ground-motion data at design level is often limited. In order to analyze seismic performance of structures, ground-motion time histories need to be either selected from recorded strong-motion database or numerically simulated using stochastic approaches. In this paper, a detailed procedure to select proper acceleration time histories from the Next Generation Attenuation (NGA) database for several cities in Taiwan is presented. Target response spectra are initially determined based on a local ground-motion prediction equation under representative deterministic seismic hazard analyses. Then several suites of ground motions are selected for these cities using the Design Ground Motion Library (DGML), a recently proposed interactive ground-motion selection tool. The selected time histories are representatives of the regional seismic hazard and should be beneficial to earthquake studies when comprehensive seismic hazard assessments and site investigations are unavailable. Note that this method is also applicable to site-specific motion selections with the target spectra near the ground surface considering the site effect.

1 Introduction

In performance-based earthquake engineering, ground-motion time histories are usually needed for analyzing the distribution of dynamic responses of nonlinear systems, such as site response or structural analysis. In such an analysis, it is one of the key aspects to use appropriate acceleration time histories, which should realistically reflect regional seismology and site conditions.

Understandably, the selected time histories should reasonably respond to seismic hazards at a given site. For example, a recent technical guideline implemented by the US Nuclear Regulatory Commission (USNRC, 2007) prescribed the probabilistic seismic hazard analysis (PSHA) as the underlying approach to generate time histories for future earthquake-resistant designs. Many studies have highlighted the importance of matching a target response spectrum in the ground-motion selection and modification process (e.g., Bommer and Acevedo, 2004). The target spectrum can be obtained by deterministic seismic hazard analysis (DSHA), PSHA, or seismic design codes. A classic example is SIMQKE, which generates synthetic time histories to match a target response spectrum with an iterative process using Gaussian random process and a time-varying modulating function (Gasparini and Vanmarcke, 1976).

Recently, some scholars have shown that a well-selected ground-motion suite should match not only the target mean, but also the variation of the target spectrum (Jayaram et al., 2011; Wang, 2011). In other words, a suite of ground motions should be selected in performance-based earthquake engineering; the resulting ground-motion suite should properly capture the statistical distribution of ground motions under the given earthquake scenario, which is commonly specified by means, standard deviations, and inherent correlations (e.g., Baker and Jayaram, 2008; Wang and Du, 2012) of a target spectrum. There are several ground-motion selection algorithms available in the literature (Baker, 2010; Jayaram et al., 2011; Wang, 2011). One of the recently proposed interactive tools is the Design Ground Motion Library (DGML), which allows for selecting a suite of modified ground motions (multiple by scale factors) on the basis of response spectral shape and the characteristics of the recordings such as magnitude, distances, faulting types, and site conditions (Wang et al., 2015).

This paper aims to present a detailed procedure in selecting ground-motion time histories for major cities of Taiwan using the DGML interactive tool. With DSHA for these cities, several suites of time histories are selected from the Pacific Earthquake Engineering Research Center's Next Generation Attenuation (NGA) strong-motion database (Chiou et al., 2008). Those selected motion suites are appropriate for general seismic designs, e.g., dynamic analysis of structures in these cities.

2 The DSHA

2.1 Overview of DSHA

Seismic hazard analysis is an approach to describe the potential shaking intensity for future earthquakes, which can be estimated by deterministic or probabilistic approaches. The deterministic approach estimates the intensity measure amplitude (e.g., peak ground acceleration (PGA) as 0.2 g) under an assigned earthquake scenario, while the probabilistic approach estimates the annual rate of exceeding the specific level of earthquake shaking at a site (e.g., PGA = 0.2 g corresponding to 10 % probability of exceedance in 50 years).

Compared to the complicated probabilistic approach, DSHA is an analysis accounting for a worst-case scenario in terms of earthquake size and location. Specifically, DSHA utilizes the maximum magnitude and shortest source-to-site distance to evaluate the ground-motion intensities under such a worse-case scenario. The basic steps are listed as follows: (1) identify all possible fault sources of earthquakes around a given site; (2) define the maximum magnitude and closest distance for each fault; (3) compute the ground-motion intensities based on attenuation relationships; (4) take the maximum intensity amplitudes as the final DSHA estimate. Figure 1 shows a schematic diagram illustrating the frame-

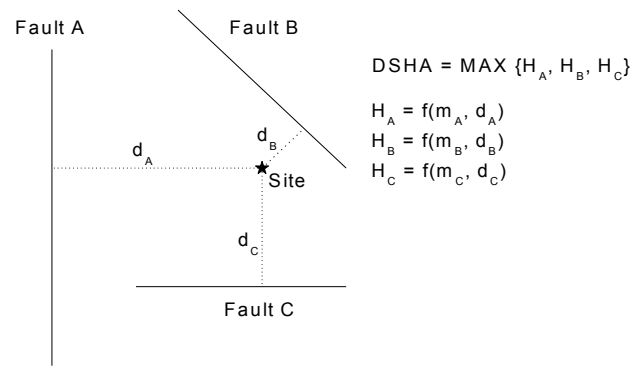


Figure 1. Schematic diagram illustrating the analytical framework of DSHA, where the solid star represents a study site, H denotes the seismic hazard induced by each source, m and d are the maximum earthquake magnitude and shortest source-to-site distance, and f is the function of a ground-motion model.

work and the algorithm for DSHA. Seismic source models, the maximum earthquake of each source, and ground-motion prediction equations (GMPEs) are key inputs for DSHA. The detailed source models and GMPEs used in this study would be introduced in this following subsection.

2.2 Seismic source model and ground-motion model

Figures 2 and 3 show the up-to-date seismic source models for Taiwan (Cheng et al., 2007), which have also been used in a few seismic hazard studies by several authors (Cheng et al., 2007). It includes 20 area sources, in addition to 49 line sources associated with each active fault on this island. Table 1 summarizes the best-estimated maximum magnitude for each source from the literature (Cheng et al., 2007). The seismic zonation used in this study (from zones A to T) is categorized as shallow crustal regional source following previous researchers' work (e.g., Tsai, 1986; Cheng, 2002; Cheng et al., 2007). The maximum earthquake magnitude reflects a combined effect of regional seismology regarding historical earthquakes, focal mechanism, and source zonation, etc. Thus, the maximum magnitude of these seismogenic zones (e.g., $M = 7.1$ for source C) is adopted as the worst-case scenario during DSHA calculations. The worst-case scenario was used for identifying the earthquake scenario considered in DSHA analysis; for each area source considered, the closest source-to-site distance is assigned accordingly, as listed in Table 3. The response spectra for major cities in Taiwan are also presented in this section with DSHA calculations.

GMPEs are commonly used to predict ground-motion intensities (e.g., PGA) as a function of earthquake magnitude, source-to-site distance, site parameters, etc. A few regional GMPE models have been developed based on local strong-motion data in Taiwan (Cheng et al., 2007; Lin et al., 2011). For example, Lin and Lee (2008) developed local GMPEs for subduction earthquakes. Considering this subduction attenu-

Table 1. Summary of maximum earthquake magnitudes (in M_w) of each seismic source around Taiwan.

Area source	Max. magnitude	Line source (active fault)	Max. magnitude	Fault mechanism
Zone A	6.5	Huangchi	7.0	Norma and sinistral
Zone B	6.5	Hsiaoyukeng	7.0	Norma and sinistral
Zone C	7.1	Sanchiao	7.0	Norma and sinistral
Zone D	7.3	Nankan	6.5	Normal and dextral
Zone E	7.3	Shuanglienpo	6.2	Reverse
Zone F	7.3	Yangmei	6.6	Reverse
Zone G	6.5	Hukou	6.9	Thrust
Zone H	7.3	Hsinchu	6.8	Thrust
Zone I	6.5	Tapingt	6.5	Thrust
Zone J	6.5	Chutung	6.5	Reverse
Zone K	6.5	Hsincheng	6.7	Thrust
Zone L	7.3	Touhuanping	6.7	Dextral
Zone M	6.5	Seztan	6.8	Reverse
Zone N	8.0	Shinchoshan	6.5	Reverse
Zone O	8.3	Tuntzechiao	6.5	Dextral
Zone P	7.8	Sanyi	6.9	Thrust
Zone Q	7.8	Chelungpu	7.7	Thrust
Zone R	7.8	Changhua	7.6	Thrust
Zone S	8.0	Tamopu-Hsuangtung	7.4	Thrust
Zone T	7.8	Shuilikeng	7.0	Thrust
		Chenyulanchi	7.0	Thrust
		Chiuchiungkeng	7.0	Thrust
		Kukeng	6.3	Sinistral
		Meishan	6.5	Dextral
		Chukou	7.5	Thrust
		Muchiliao	7.1	Thrust
		Liuchia	7.1	Thrust
		Tsochen	6.4	Sinistral
		Hsinhua	6.4	Dextral
		Houchiali	6.4	Thrust
		Hsiaokangshan	6.5	Reverse
		Chishan	7.3	Thrust
		Yuchang	6.4	Reverse
		Yenwu	6.7	Reverse
		Fenshan	6.7	Reverse
		Liukuei	6.7	Reverse
		Chaochou	7.3	Reverse
		Hengchun	7.2	Reverse
		Ilan	6.9	Normal
		Chiaoichi	6.8	Normal
		Lishan	6.9	Normal
		Meilun	7.3	Norma and sinistral
		Ueimei	7.5	Norma and sinistral
		Yuli	7.5	Norma and sinistral
		Chihshang	7.3	Norma and sinistral
		Yuli west	7.3	Norma and sinistral
		Luyeh	6.9	Reverse
		Lichi	7.1	Norma and sinistral
		Chimei	7.2	Norma and sinistral

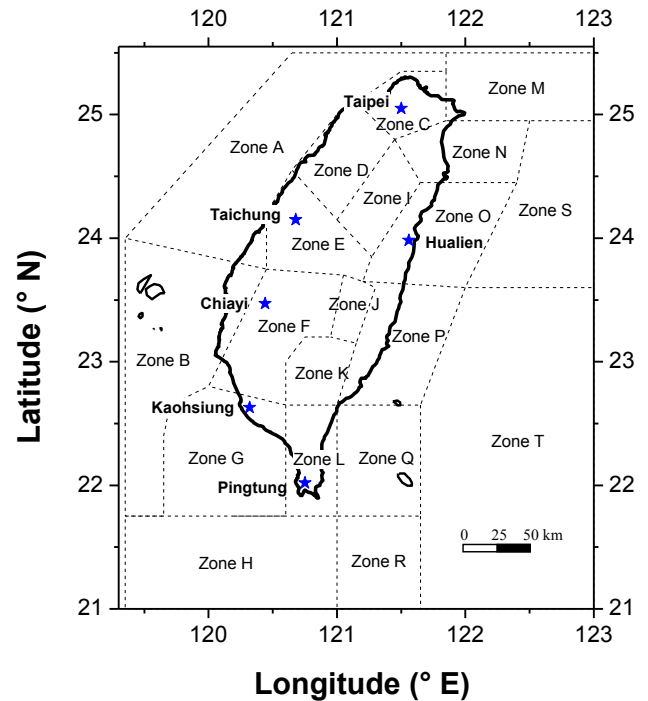


Figure 2. The area seismic source model for Taiwan (after Cheng et al., 2007); six study cities – (a) Taipei, (b) Kaohsiung, (c) Taichung, (d) Chiayi, (e) Pingtung, and (f) Hualien – are plotted as blue stars.

ation relation is incompatible with the NGA database which primarily contains records from shallow crustal earthquakes, the model is not adopted in the current study. In contrast, the recent GMPE developed by Lin et al. (2011) is capable of predicting PGA and response spectra for periods ranging from 0.01 to 5 s, and therefore it is adopted in this study to develop the target response spectra for selecting earthquake time histories.

The function form of the adopted model (Lin et al., 2011) is expressed as follows:

$$\ln Y = c_1 + c_2 M_w + c_3 \ln \left(R + c_4 e^{c_5 M_w} \right) \quad \sigma_{\ln Y} = \sigma^*, \quad (1)$$

where Y denotes PGA or spectral accelerations in unit of g , M_w refers to moment magnitude, R is the rupture distance (closest distance from the rupture surface to site) in kilometers, and c_1 to c_5 are regressed coefficients. The model's coefficients are summarized in Table 2, and $\sigma_{\ln Y}$ denotes the model's standard deviation. It is noted that this model was developed using around 5000 earthquake records, 98 % of which are taken from Taiwan. It should be also noted that the attenuation adopted in this study is for the hanging-wall and rock sites. It is agreeable that the worst-case scenarios considered in this paper may not be the hanging-wall case. However, since the Lin et al. (2011) model is the only available regional-specific response spectral attenuation model for shallow crustal earthquakes to the authors' best knowledge,

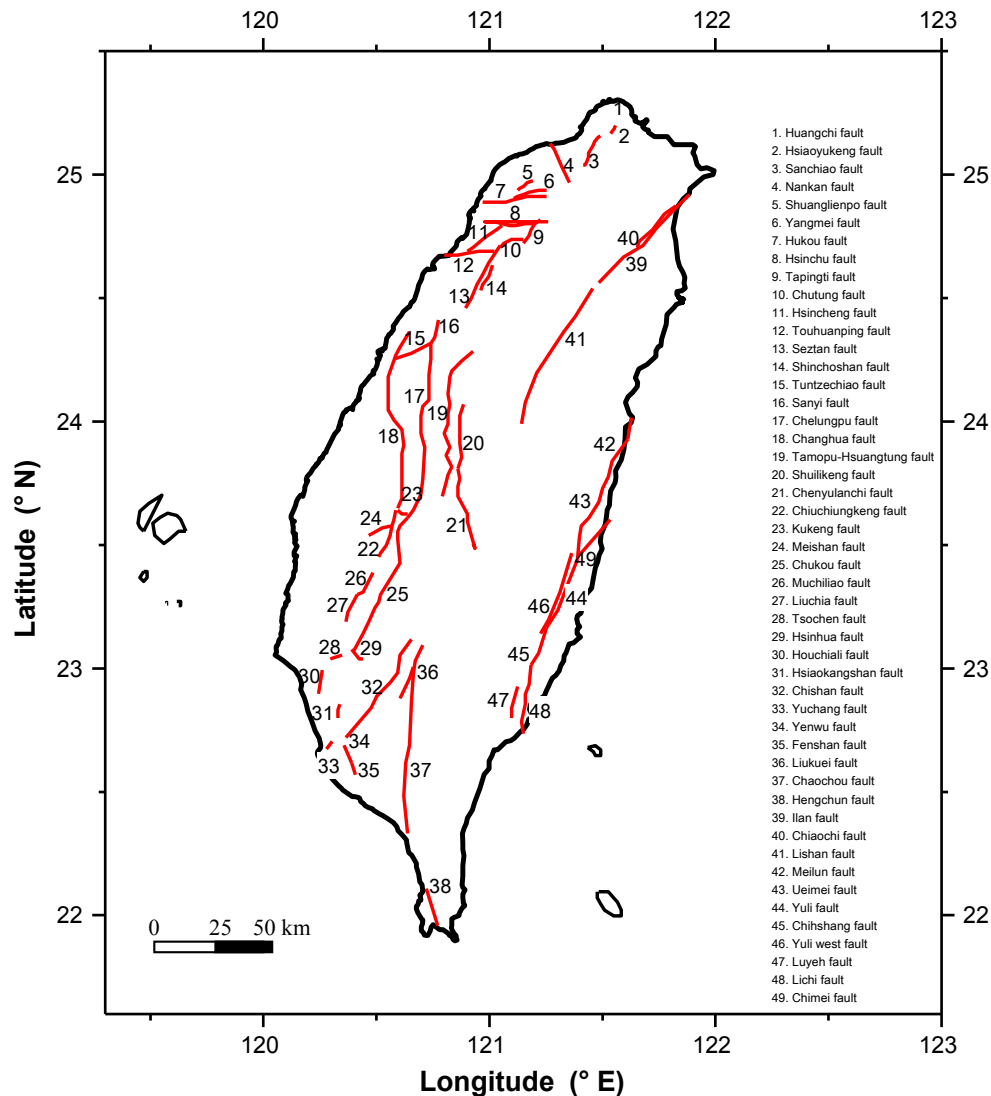


Figure 3. The line source model of the active faults in Taiwan (Cheng et al., 2007).

this hanging-wall attenuation model is adopted in the current study to construct the target response spectra with reasonably conservative results provided.

It is also worth noting that we only employ the local ground-motion model in this study. It is understood that logic-tree analyses can be used to quantify the so-called epistemic uncertainty in PSHA. As studied by some scholars (e.g., Krinitzsky, 2003), however, the weights in logic-tree analyses cannot be scientifically verified. Therefore, this study used one local model available as the best estimate. When new local models are developed, an update of seismic hazards or sensitivity analyses will be worth conducting in the future.

2.3 DSHA-based response spectra

The aforementioned DSHA procedures can be performed for major cities in Taiwan, with the adopted seismic source models (Figs. 2 and 3) and attenuation relationship introduced in previous subsections. Six major cities are chosen for such calculations: site a, Taipei; site b, Kaohsiung; site c, Taichung; site d, Chiayi; site e, Pingtung; and site f, Hualien. Figure 2 shows location of the six study sites, with their coordinates (i.e., the city's geographical centers) summarized in Table 3. As Taiwan is located at the boundary between the Philippine Sea Plate to the east and the Eurasian Plate to the west, the six study sites are intentionally selected to represent a variety of geological components of the island: sites a, c, and d are located at the western foothills, mainly composed of Oligocene to Pleistocene clastic sediments, where synoro-

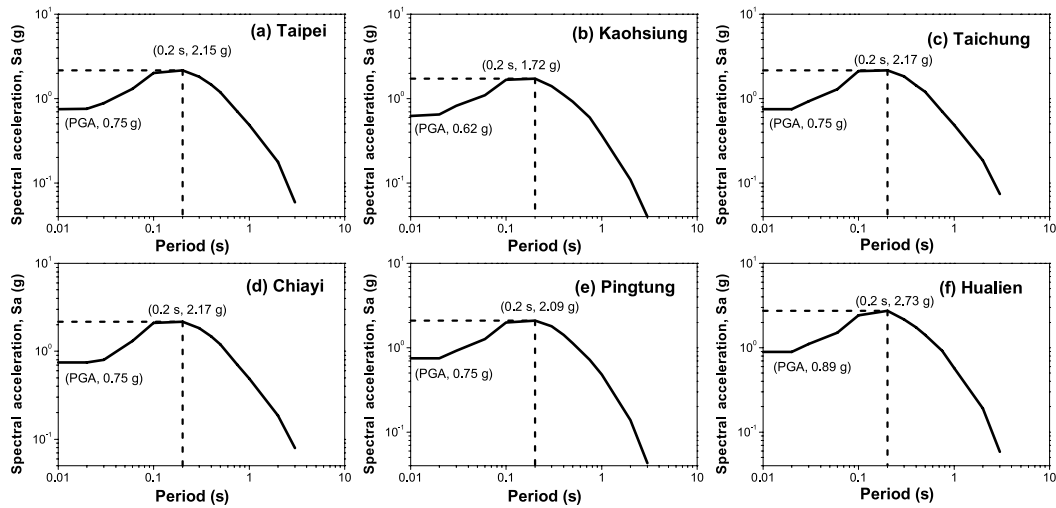


Figure 4. The response spectra for major cities in Taiwan with DSHA calculations.

Table 2. Summary of the coefficients of the local ground-motion models used in this study (Lin et al., 2011).

Periods (s)	c_1	c_2	c_3	c_4	c_5	$\sigma_{\ln Y}$
PGA	-3.279	1.035	-1.651	0.152	0.623	0.651
0.01	-3.253	1.018	-1.629	0.159	0.612	0.647
0.06	-1.738	0.908	-1.769	0.327	0.502	0.702
0.09	-1.237	0.841	-1.750	0.478	0.402	0.748
0.1	-1.103	0.841	-1.765	0.455	0.417	0.750
0.2	-2.767	0.980	-1.522	0.097	0.627	0.697
0.3	-4.440	1.186	-1.438	0.027	0.823	0.685
0.4	-5.630	1.335	-1.414	0.014	0.932	0.683
0.5	-6.746	1.456	-1.365	0.006	1.057	0.678
0.6	-7.637	1.557	-1.348	0.0033	1.147	0.666
0.75	-8.641	1.653	-1.313	0.0015	1.257	0.652
1	-9.978	1.800	-1.286	0.0008	1.377	0.671
2	-12.611	2.058	-1.261	0.0005	1.497	0.706
3	-13.303	2.036	-1.234	0.0013	1.302	0.702

genic sediments of the foreland basin have been accreted and deformed. Site b is located at the coastal plain as a part of the foreland basin of Taiwan. Site e is located in the southern part of the Central Mountain Range with mostly Miocene to Eocene slates, corresponding to the area of highest altitudes in Taiwan. Site f is located at the Longitudinal Valley, which is believed to be the suture zone between the Luzon arc and the Chinese continental margin (CES, 2017). For each study site, the worse-case scenario was firstly identified, and then the corresponding response spectrum was determined by using the adopted local GMPE.

Figure 4 shows the resulting response spectra from DSHA calculations for the six considered cities in Taiwan. Table 3 also summarizes the controlling seismic source for each site. For example, the DSHA seismic hazard at the center of site a is governed by Area Source C. In other words, Area

Source C, rather than the other line sources or active faults, contributes to the deterministic seismic hazard for the center of Taipei. The same situation is occurring to other cities with an area source being the controlling source. This is expected because the DSHA seismic hazard from an area source could be commonly higher than a line source due to the relatively closer source-to-site distance.

It should be noted that the adopted local GMPE has been thoroughly compared with the globally NGA GMPEs (Abrahamson and Silva, 2008; Boore and Atkinson, 2008; Campbell and Bozorgnia, 2008; Chiou and Youngs, 2008). In general, the PGA amplitudes predicted by the adopted model are generally comparable to those of the NGA models, except that for scenarios with distances greater than 20 km the estimated PGAs of the local model attenuate faster. The steeper slope of the local attenuation curves could be due to the fact that the local crust is relatively weak, given that Taiwan is a very young orogeny (Lin et al., 2011). This implies that a design or target spectrum derived from local GMPEs is particularly necessary for selecting suitable ground-motion time histories for local engineering practice.

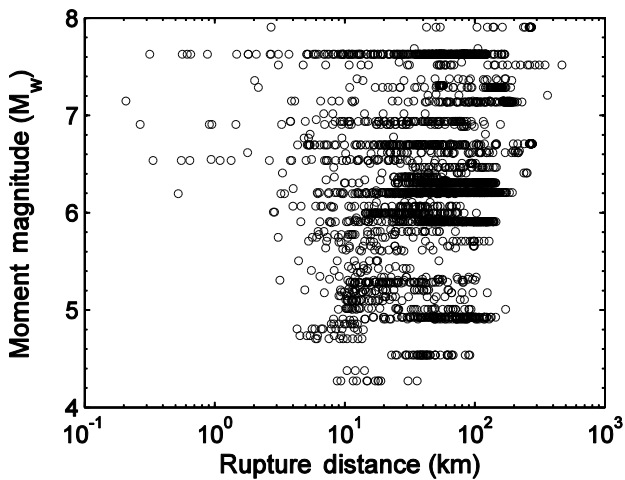
3 Selection of ground-motion time histories

3.1 The NGA database and DGML

The source for ground-motion selection in this study is the PEER-NGA strong motion database, which contains 3551 three-component recordings from 173 earthquakes (Chiou et al., 2008). Various subsets of the database have been used to develop GMPE models for various ground-motion intensities in earthquake engineering (e.g., Du and Wang, 2013; Foulser-Piggott and Stafford, 2012). Figure 5 shows the moment magnitude–rupture distance distribution of the ground motions in the NGA database. The aforementioned interac-

Table 3. Summary of the sites' coordinates, along with respective controlling seismic sources for each site in DSHA computations.

City	Latitude (° N)	Longitude (° E)	Controlling source	Maximum magnitude	Closest source-to-site distance (km)
(a) Taipei	25.05	121.50	Zone C	7.1	2
(b) Kaohsiung	22.63	120.32	Zone G	6.5	2
(c) Taichung	24.15	120.68	Zone E	7.3	2
(d) Chiayi	23.47	120.44	Zone F	7.3	2
(e) Pingtung	22.02	120.75	Zone L	7.3	2
(f) Hualien	23.98	121.56	Zone O	8.3	2

**Figure 5.** Moment magnitude and rupture distance distribution for PEER NGA records used in this study.

tive tool, DGML, is used to search ground-motion time histories in the NGA database on the basis of similarity of a record's response spectrum to the target response spectrum over a user-defined range of period (Wang et al., 2015). The DGML has the broad capability to search for ground-motion time histories in the library database on the basis of response spectral shape, characteristics of the recordings in terms of earthquake magnitude and type of faulting distance, site characteristics, duration, and presence of velocity pulses in near-fault time histories. These ground-motion intensity measures have been found to be important in liquefaction and seismic assessment of a variety of geotechnical systems (Du and Wang, 2014; Huang and Wang, 2015a, b, 2017; Wang and Wei, 2016; Ye and Wang, 2015, 2016; Zhang and Wang, 2016). The DGML Search Engine window is shown in Fig. 6. It contains the following major parts: (1) inputs for searching criteria, (2) prescribed range of scale factor, (3) prescribed weight factor for spectral period, (4) spectrum plot of selected motions, (5) MSE (mean squared error) of each individual selected ground-motion record, (6) scale factor of each record, (7) event name, and (8) station name of each record.

To be more specific, the seismological parameter bounds (e.g., range of considered M_w and distance R) are needed as inputs, which can implicitly constrain the ground-motion characteristics in addition to the explicit target spectrum. Given the fact that the target spectra from DSHA are a result of the maximum earthquake and the closest source-to-site distance, a relatively large magnitude bound ($5.5 < M_w < 8$) and a narrow distance range ($0 \text{ km} < R_{\text{rup}} < 30 \text{ km}$) have been employed as the searching criteria. Since all six cities are located at soil sites, a V_{s30} (time-averaged shear-wave velocity down to 30 m) bound in the range of $0\text{--}450 \text{ m s}^{-1}$ is also applied. Other causal parameters, such as the category of fault types or the range of duration parameters, are not particularly specified.

Scaling factor is another key input for selecting ground motions but has been subjected to intense debate over the past decades. Previous researchers pointed out that improper scaling of a record can lead to bias estimates of structural responses (Luco and Cornell, 2007). For example, if an excessive range of scale factors is applied, the selected ground-motion suite might result in drastically biased distribution of the other ground-motion characteristics, such as duration and Arias intensity, which cannot be represented by the target response spectrum. Therefore, we follow the general practice of the DGML and assign a relative narrow range of scale factors ($0.4\text{--}2.5$) throughout the selection procedure in this study (Wang et al., 2015). After searching for properly matched time histories with target spectrum and magnitude and distance thresholds, the ranking of earthquake motions is tabulated after spectral matching process. The motions of interest can be downloaded from the list, as well as their descriptions such as fault types, earthquake magnitudes, rupture distances, durations, scaling factors, and V_{s30} values (V_{s30} is commonly employed site condition indicator). Note that DGML is also capable of performing weight matching when a specific range of the motion's frequencies is of more interest in follow-up applications.

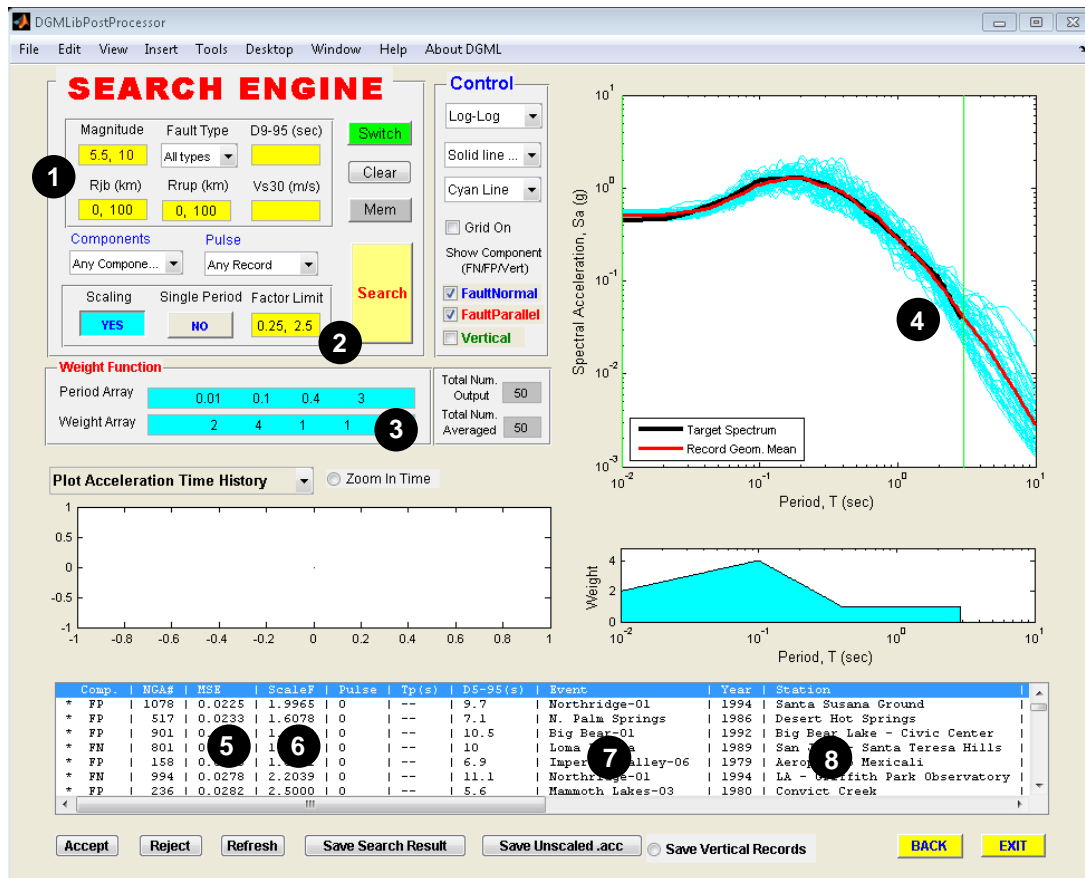


Figure 6. The screenshot of the DGML searching interface: (1) searching criteria, (2) prescribed range of scale factor, (3) prescribed weight factor for spectral period, (4) spectrum plot of selected motions, (5) mean squared error of each individual selected ground-motion record, (6) scale factor of each record, (7) event name of each record, and (8) station name of each record.

3.2 Time history recommendations for dynamic analyses of structural and geotechnical systems

With the target spectra from DSHA calculations, the selection procedures in DGML are performed to select a suite of time histories from the NGA database for each city. The DGML search engine adopted in this study searches the NGA database for ground-motion waveforms that satisfy the general criteria (i.e., $5.5 < M_w < 8$, $0 < R_{rup} < 30$ km) and then ranks these records in an order of an increasing MSE. It means that the ground-motion waveform that matches the target response spectrum best has the lowest MSE and will be ranked as no. 1. To be more specific, the MSE is defined using the following equation (Wang et al., 2015):

$$MSE = \frac{\sum_i w(T_i) \{ \ln(Sa^{target}(T_i)) - \ln(f \cdot Sa^{record}(T_i)) \}^2}{\sum_i w(T_i)}, \quad (2)$$

where $Sa(T_i)$ denotes the spectral acceleration at spectral period T_i , $w(T_i)$ denotes a weight function that allows for assigning weights to different period ranges so that the periods

of more interest can be emphasized in the ground-motion selection process, and f represents a scale factor to linearly scale the whole ground-motion time history. It should be also noted that the MSE does not vary too much in some cases. For example, as shown in Fig. 6, the MSE ranges from 0.023 to 0.035, indicating that the selected scaled ground motions are almost equally good and compatible with the target response spectrum. Therefore, in this study, we intentionally select different ground-motion waveforms for another study site if some have been already recommended. We expect that, by doing so, more flexibility and options can be provided for time history analyses in engineering practice. It should also be noted that although different ground motions are selected for various sites, they are statically consistent and compatible with the corresponding DSHA spectrum.

Figure 7 shows the selected response spectra for the six study cities. The median and median ± 1 standard deviation of the selected spectral acceleration ordinates are also compared to the target spectrum in each plot. It can be seen that the selected ground-motion suites can properly match the target spectra over a wide period range. Table 4 sum-

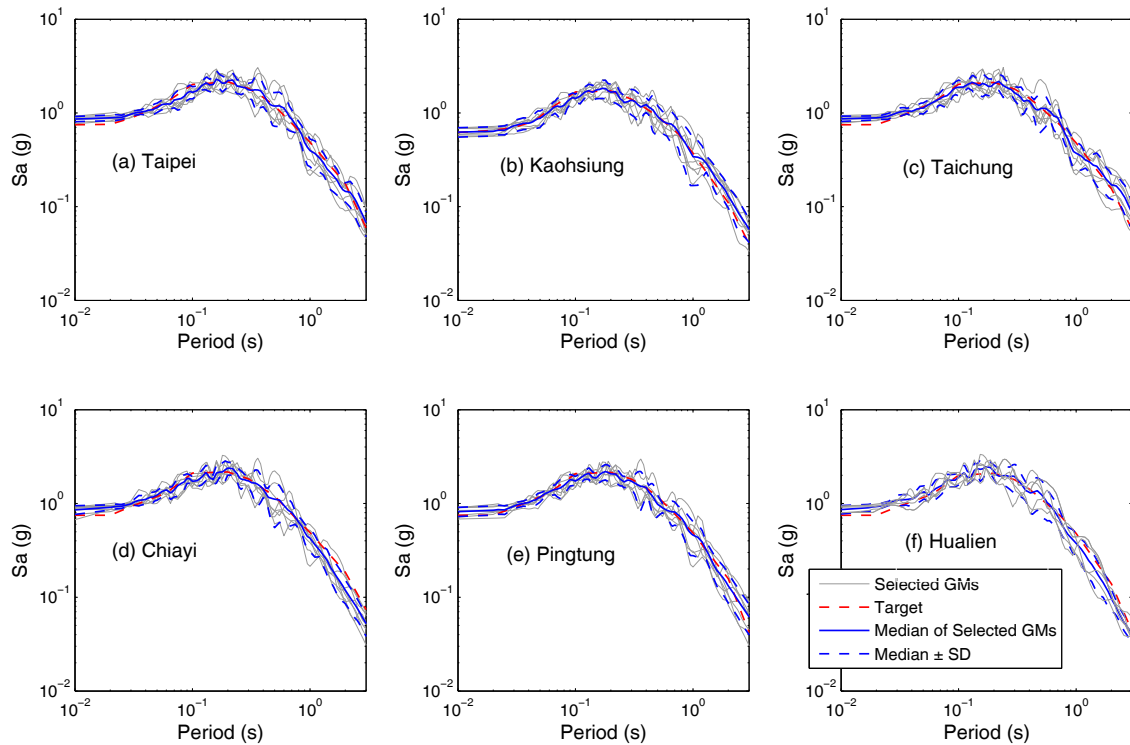


Figure 7. The target spectrum, individual and average response spectrum of selected records for six major cities in Taiwan.

marizes the time histories selected from the database. Figures 8–14 show the selected time histories for the six cities in Taiwan with seismic hazards calculated with DSHA calculations. Note that two sets of selections were given for site a, with and without the consideration of basin effect. It should also be noted that for each site the best-matching motions were selected regardless of local earthquakes or not, in addition to one or two best-matching local motion (i.e., the Chi-Chi earthquake). The multiple time histories in each suite are considered as a measure to account for the variability or natural randomness of ground-motion characteristics under a considered scenario, which, for example, is considered as mandatory for probabilistic site response analyses prescribed in a technical reference (USNRC, 2007).

4 Discussions

4.1 DSHA versus PSHA

PSHA and DSHA are the two representative approaches in assessing earthquake hazards. Over the past decades, numerous seismic hazard studies have been conducted with the two methods (e.g., Joshi et al., 2007; Kolathayar and Sitharam, 2012; Moratto et al., 2007; Sitharam and Vipin, 2011; Stirling et al., 2011). The two methods have also been prescribed in various technical references. As mentioned previously, a technical reference (USNRC, 2007) prescribes PSHA as the

underlying approach, in contrast to another guideline implemented by California Department of Transportation prescribing DSHA for bridge designs under earthquake loadings (Mualchin, 2011).

It is worth noting that extensive discussions over the pros and cons of the two methods have been reported in the literature (e.g., Bommer, 2003; Castanos and Lomnitz, 2002; Krinitzsky, 2003; Klugel, 2008). In general, DSHA is a simple approach that earthquake scenarios are considered logically understandably, but the uncertainties in DSHA may not be well quantified. In contrast, PSHA is capable of quantifying the uncertainties associated with earthquake scenarios via a probabilistic approach; however, some scholars (e.g., Krinitzsky, 2003) have pointed out the shortcomings in PSHA, such as the uniform assumption in the occurrences of earthquakes. It is not this paper's purpose to argue which seismic hazard method is superior. With all that in mind, however, it is clear that both the deterministic and probabilistic analysis are needed and useful in engineering applications. The use of the DSHA approach in this study is primarily due to its analytical simplicity and transparency. Since it has been reported that DSHA rather than PSHA is more appropriate for design of critical structures (Bommer et al., 2000), the selected ground-motion suites, with a representative seismic hazard analysis and a reputable earthquake database, are then recommended for such applications.

Table 4. Summary of the earthquake time history recommendations from the NGA database with DSHA calculations.

City	Earthquake motion	Year	Magnitude	Rupture distance (km)	Station	Fault mechanism	D_{5-95} (s)	V_{s30} (m s^{-1})	Scale factor	MSE
Taipei	Mammoth Lakes-01	1980	6.06	4.0	Convict Creek	N–O ^c	9.1	338	1.67	0.023
	Coalinga-05	1983	5.77	16.1	Pleasant Valley P.P.-FP	Reverse	5.0	257	1.93	0.023
	N. Palm Springs	1986	6.06	6.0	Whitewater Trout Farm	R–O ^b	5.1	345	1.67	0.023
	N. Palm Springs	1986	6.06	11.2	North Palm Springs	R–O ^b	5.6	345	1.48	0.030
	Coalinga-05	1983	5.77	16.1	Pleasant Valley P.P.-FN	Reverse	5.0	257	2.00	0.031
	Imperial Valley-06	1979	6.53	2.7	Bonds Corner	Reverse	9.7	223	1.05	0.031
	Northridge-01	1994	6.69	28.3	LA – Centinela St.	Reverse	13.0	235	0.98	0.031
	N. Palm Springs	1986	6.06	6.0	Whitewater Trout Farm	R–O ^b	5.1	345	1.52	0.032
Taipei (with basin effect)	Northridge-01	1994	6.69	14.7	Canoga Park	Reverse	11.1	268	0.50	0.030
	Chi-Chi	1999	7.62	10.0	CHY101	R–O ^b	29.0	259	1.16	0.033
	Northridge-01	1994	6.69	28.3	LA – Centinela St.	Reverse	13.0	235	0.98	0.039
	Coalinga-01	1983	6.36	8.4	Pleasant Valley P.P.	Reverse	8.0	257	1.32	0.039
	Loma Prieta	1989	6.93	15.2	Capitola	R–O ^b	14.7	289	1.50	0.039
	Coalinga-05	1983	5.77	16.1	Pleasant Valley P.P.	Reverse	5.0	257	1.22	0.041
	Imperial Valley-06	1979	6.53	2.7	Bonds Corner	Strike–slip	9.7	223	1.35	0.041
	M. - N.*-01	1972	6.24	4.1	Managua-ESSO	Strike–slip	9.0	289	2.00	0.043
Kaohsiung	Big Bear-01	1992	6.46	9.4	Big Bear Lake	Strike–slip	10.5	338	1.88	0.025
	Whittier Narrows-01	1987	5.99	14.5	Garvey Res	R–O ^b	5.9	468	2.02	0.027
	Loma Prieta	1989	6.93	10	Gilroy Gavilan College	R–O ^b	4.7	729	1.66	0.027
	Coalinga-05	1983	5.77	16.1	Pleasant Valley P.P.	Reverse	4.9	257	1.54	0.029
	N. Palm Springs	1986	6.06	6.8	Desert Hot Springs	R–O ^b	7.1	345	2.03	0.029
	Loma Prieta	1989	6.93	14.7	Santa Teresa Hills	R–O ^b	10	271	2.03	0.030
	Mammoth Lakes-01	1980	6.06	4	Convict Creek	N–O ^c	9.1	338	1.30	0.030
	N. Palm Springs	1986	6.06	11.2	North Palm Springs	R–O ^b	5.6	345	1.19	0.031
Taichung	Mammoth Lakes-01	1980	6.06	6.6	Convict Creek	N–O ^c	9.1	338	1.69	0.030
	Coalinga-05	1983	5.77	16.1	Pleasant Valley P.P.-FP	Reverse	4.9	257	1.96	0.034
	Coalinga-05	1983	5.77	16.1	Pleasant Valley P.P.-FN	Reverse	5.0	257	1.99	0.040
	Northridge-01	1994	6.69	28.3	LA – Centinela St.	Reverse	11.9	235	1.99	0.041
	N. Palm Springs	1986	6.06	16.1	North Palm Springs	R–O ^b	5.6	345	1.51	0.041
	Northridge-01	1994	6.69	22.5	LA-UCLA	Reverse	9.4	398	2.00	0.041
	N. Palm Springs	1986	6.06	6.0	Whitewater Trout Farm	R–O ^b	25.8	345	1.70	0.043
	Loma Prieta ^d	1989	6.93	12.8	Gilroy Array no. 3	R–O ^b	7.7	349	1.63	0.045
Chiayi	Coalinga-05	1983	5.77	2.7	Pleasant Valley P.P.	Reverse	4.9	257	1.92	0.032
	Mammoth Lakes-01	1980	6.06	6.6	Convict Creek	N–O ^c	9.1	338	1.66	0.034
	N. Palm Springs	1986	6.06	6.0	Whitewater Trout Farm	R–O ^b	5.1	345	1.67	0.039
	Whittier Narrows-01	1994	6.69	28.3	LA – Obregon Park	R–O ^b	7.8	349	2.00	0.040
	Loma Prieta	1989	6.93	17.5	WAHO	R–O ^b	11.1	376	1.30	0.045
	Coalinga-05 ^d	1983	5.77	8.5	Oil City	Reverse	2.8	376	1.03	0.046
	Imperial Valley-06	1979	6.53	2.7	Bonds Corner	Reverse	9.7	223	1.04	0.046
	Chi-Chi-03	1989	6.2	7.6	TCU078	Reverse	6.7	443	1.66	0.046
Hualien	Mammoth Lakes-01	1980	6.06	6.6	Convict Creek	N–O ^c	9.1	338	2.01	0.035
	N. Palm Springs	1986	6.06	6.0	Whitewater Trout Farm	R–O ^b	5.1	345	2.00	0.035
	Imperial Valley-06	1979	6.53	2.7	Bonds Corner	Reverse	9.7	223	1.26	0.036
	Chi-Chi-03	1989	6.2	7.6	TCU078	Reverse	6.7	443	2.00	0.036
	Coalinga-05 ^d	1983	5.77	8.5	Oil City	Reverse	2.8	376	1.24	0.038
	Superstition Hills-02	1987	6.54	5.6	Superstition Camera	Strike–slip	12.1	362	1.53	0.038
	Loma Prieta ^d	1989	6.93	12.8	Gilroy Array no. 3	R–O ^b	7.7	349	1.92	0.040
	Chi-Chi-06	1989	6.3	10.1	TCU079	Reverse	4.0	443	1.28	0.040
Pingtung	Imperial Valley-06	1979	6.53	0.3	Aeropuerto Mexicali	Strike–slip	7.1	274	2.02	0.023
	Imperial Valley-06	1979	6.53	3.9	EL Centro Array no. 8	Strike–slip	5.8	206	1.38	0.028
	Coalinga-01	1983	6.36	8.4	Pleasant Valley P.P.	Reverse	8.0	257	1.30	0.029
	Coalinga-05	1983	5.77	16.1	Pleasant Valley P.P.	Reverse	5.0	257	1.50	0.032
	Coalinga-05	1983	5.77	23.5	Bonds Corner	Reverse	5.0	257	1.26	0.033
	Northridge-01	1994	6.69	15.6	Tarzana, Cedar Hill A	Reverse	10.3	257	2.00	0.034
	Chi-Chi	1999	7.62	10.0	CHY101	R–O ^b	29.0	258	1.59	0.035
	Loma Prieta	1989	6.93	15.2	Capitola	R–O ^b	14.7	288	1.43	0.035

^a M–N: Managua–Nicaragua. ^b R–O: reverse–oblique. ^c N–O: normal–oblique. ^d Refers to pulse-like record.

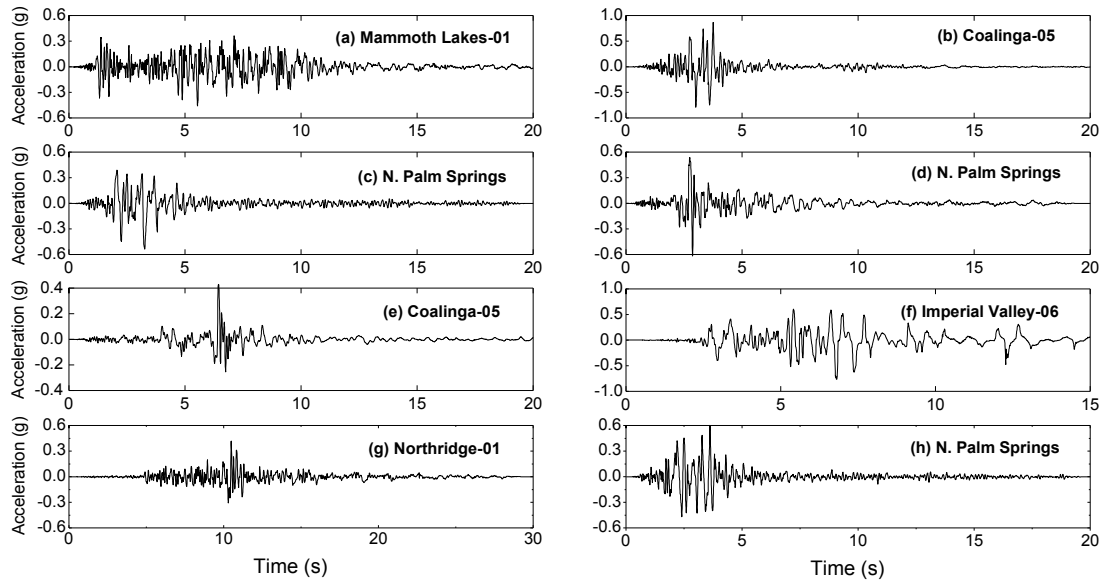


Figure 8. Eight time history recommendations for Taipei (site a) with DSHA calculations and the NGA strong-motion database.

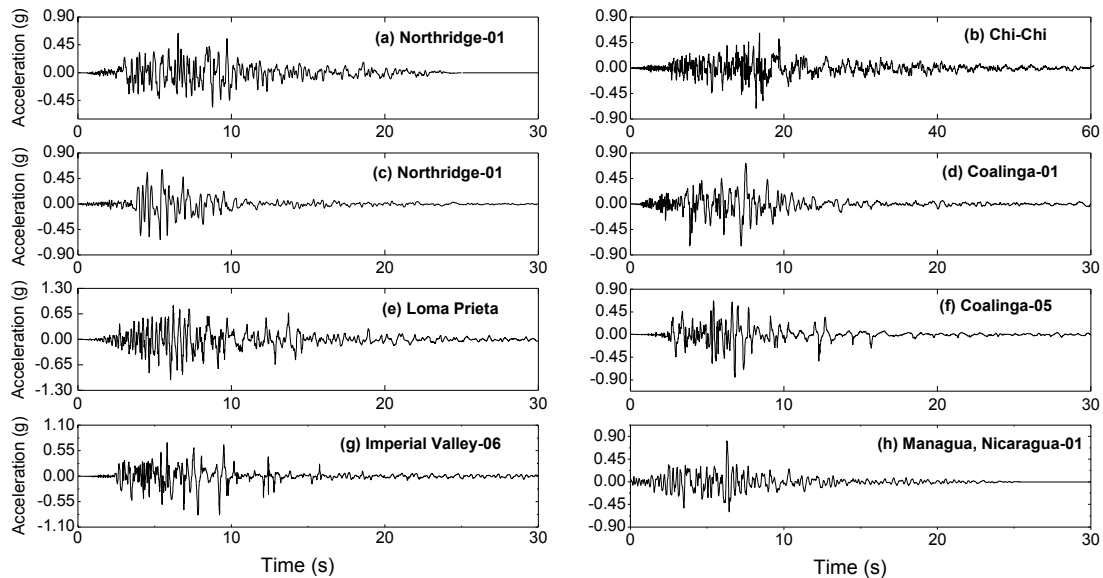


Figure 9. Another set of time history recommendations for Taipei (site a) with the basin effect taken into account.

4.2 Site-specific time histories

This paper presents an option to select earthquake time histories from the reputable NGA database. Strictly speaking, those time history recommendations are not site specific, because the site condition is not carefully taken into account with a comprehensive site investigations and site response analyses. In other words, the site-specific motions are those from seismic hazard analyses to site response studies.

As a result, this study refers to those time history recommendations as “tentative site-specific”, because the site effect

is comprehensively characterized not with a more detailed site response analysis but with a soil-site GMPEs. Therefore, the selected ground-motion time histories could be recommended for general earthquake analytical cases, where specific site investigations are not performed. Since the recommended time histories can reasonably reflect the local seismic hazards at these cities, they should be used as basic results and then be serviceable for common engineering practice.

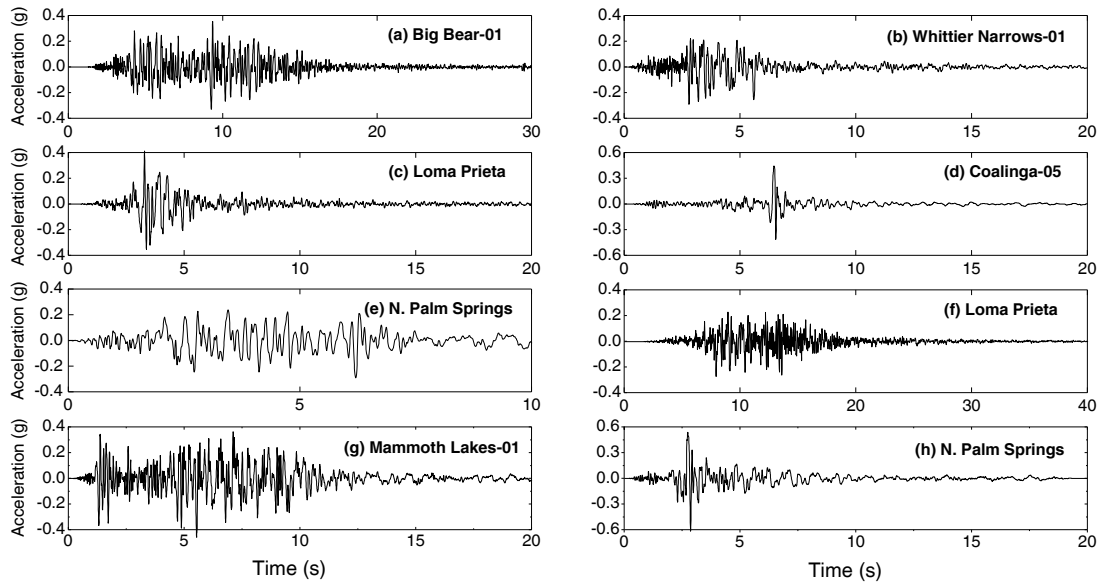


Figure 10. Eight time history recommendations for Kaohsiung (site b) with DSHA calculations and the NGA strong-motion database.

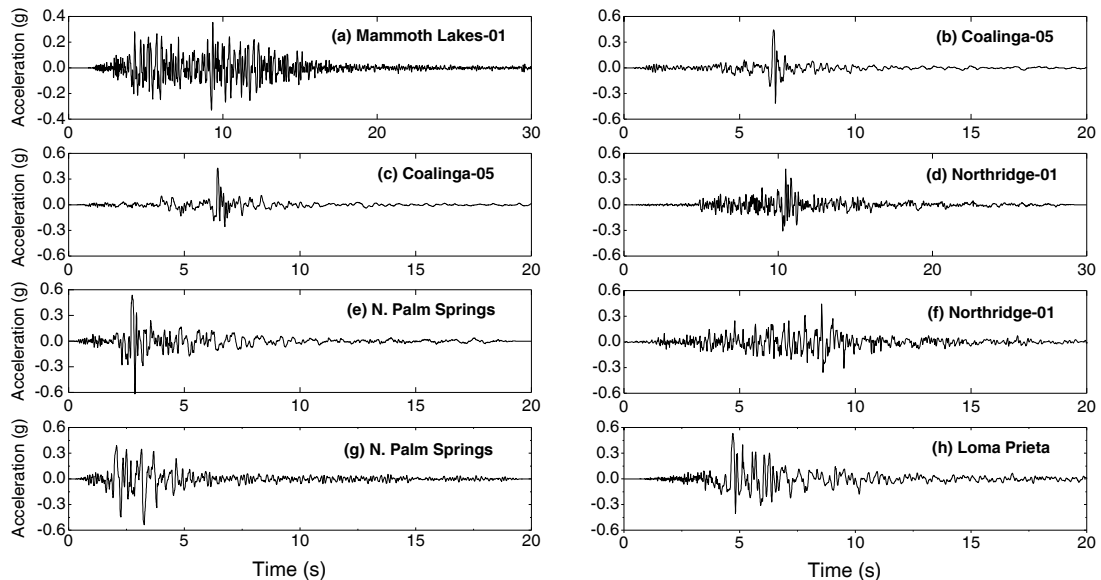


Figure 11. Eight time history recommendations for Taichung (site c) with DSHA calculations and the NGA strong-motion database.

4.3 Basin effect

Basin effect is another important issue to estimate the seismic hazards for site a. From analyzing the recorded time histories around Taipei (Sokolov et al., 2009, 2000), some suggestions were made to up-scale low-frequency spectral accelerations to incorporate the basin effect in Taipei. Following this suggestion, Fig. 15 shows the response spectra with/without considering basin effects for Taipei by DSHA calculations. Likewise, the time histories matching the up-scaled spectra (with

basin effects) as the target are selected from the database, as summarized in Table 4.

4.4 Why are local earthquake’s motions not selected for all cases?

It may come as a surprise that the motions of the local earthquake were “out-performed” by non-local motions in matching the response spectra with local ground-motion models. This might be due to the following reasons. First, apart from the Chi-Chi earthquake, most events used for developing the

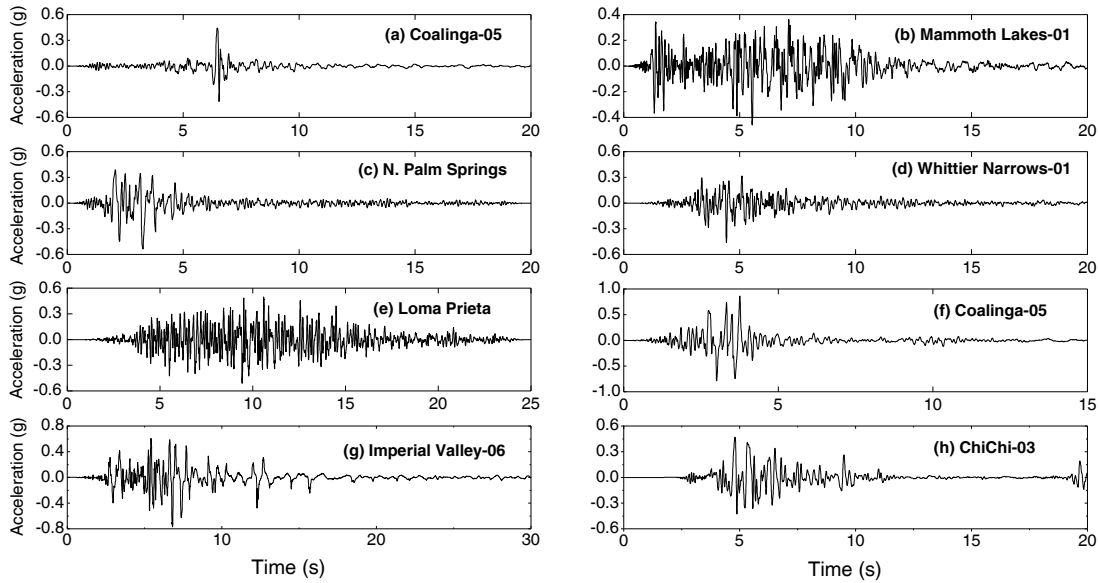


Figure 12. Eight time history recommendations for Chiayi (site d) with DSHA calculations and the NGA strong-motion database.

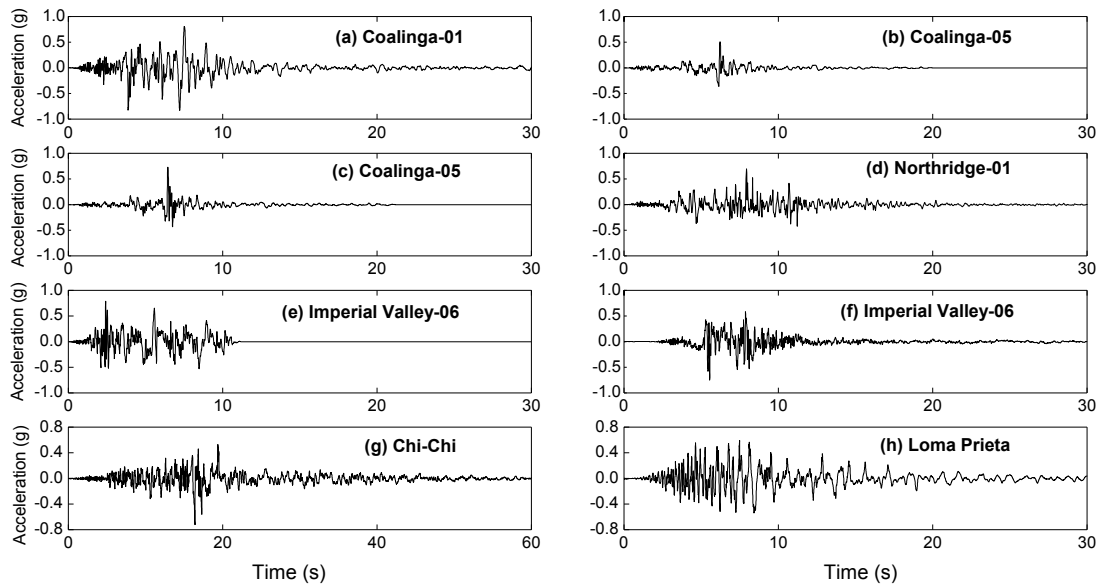


Figure 13. Eight time history recommendations for Pingtung (site e) with DSHA calculations and the NGA strong-motion database.

local GMPE are not included in the NGA database. Additionally, the employed searching process does not specify more weights or preferences to local earthquakes. As discussed previously, the search criterion are only associated with the spectral shape and seismological parameters such as magnitude, distance, and site condition. The search engine searches the database and ranks the records based on a quantitative measure: the MSE. Table 4 summarizes MSE for each single selected record. It can be observed that the MSEs range from 0.023 to 0.046 for different study sites. These ground-motion waveforms have been recommended

in this study based on their compatibility with the target response spectrum, and such compatibility is parameterized as the MSE. It is agreeable that local ground motions may contain intrinsic correct path effects at the site of interest. However, the principle of current ground-motion selection practice is searching for time history record sets in the database on the basis of the similarity of a record's response spectral shape to a design response spectrum over a user-defined period range. In such a case, local earthquake records are not always selected and recommended for the study sites because they might not conform to the target spectra. With this in

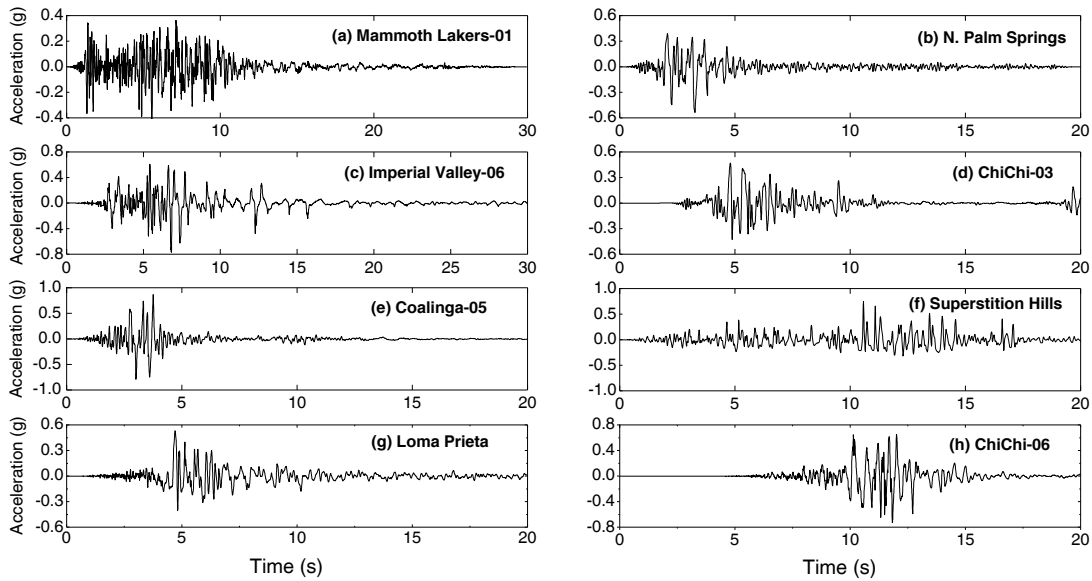


Figure 14. Eight time history recommendations for Hualien (site f) with DSHA calculations and the NGA strong-motion database.

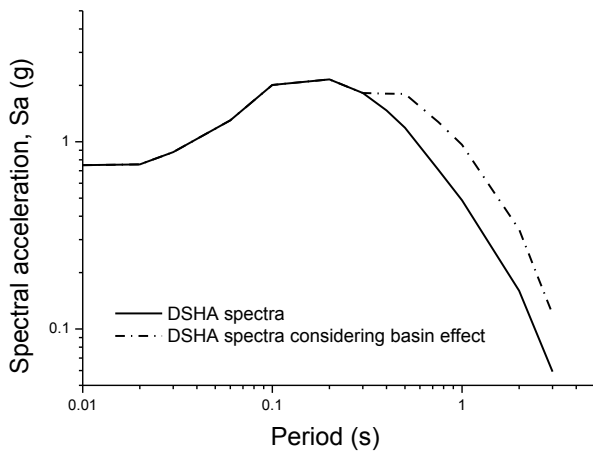


Figure 15. The basin effect in Taipei (site a) on response spectra; the spectra scaling follows the suggestions of Solokov et al. (2009, 2010).

mind, as long as the size of the database is sufficient, it is not surprising that a non-local ground motion can better match the target spectra.

It is also worth mentioning that the local GMPE adopted in this study is a “generalized” one and is primarily consistent with global GMPEs in terms of spectral shape and response acceleration amplitudes. Figure 16 compares spectral accelerations predicted using the local model with those computed using other four widely used NGA global GMPEs, namely, AS08, BA08, CB08, and CY08, for several earthquake scenarios (Abrahamson and Silva, 2008; Boore and Atkinson, 2008; Campbell and Bozorgnia, 2008; Chiou and Youngs, 2008). It can be seen that under an earthquake scenario of

$M = 7$, $R_{rup} = 30$ km, and $V_{s30} = 760$ m s⁻¹, the spectral accelerations predicted by local attenuation agree well with the BA08 and CY08 models across a wide range of periods (i.e., from 0.01 to 5 s). As for the scenarios of $M = 7$, $R_{rup} = 10$ km, and $V_{s30} = 760$ m s⁻¹, the spectral accelerations predicted by local GMPE again corresponds well with those computed using the CY08 model, as demonstrated in Fig. 16a. Apart from the consistency with global GMPEs, it is also worth mentioning that the functional form of the local model is based on Campbell (1981), which is a quite generic and widely adopted one. Therefore, in this study, ground motions that are selected from the comprehensive NGA database based on compatibility with the target response spectra can be either local or global records but not necessarily local motions, given the “generic target GMPE”.

5 Conclusions

The paper presents a simple procedure to select ground-motion time histories with target response spectra for DSHA from the NGA database using the recently proposed DGML search engine. The worst-case earthquake scenarios have been first determined for several major cities in Taiwan as a case study, and the response target spectra were computed by employing a region-specific attenuation model under the deterministic seismic hazard assessment scheme. A suite of time histories are then selected for each city by matching the computed target spectra. The selected time history suites can be recommended for general earthquake analytical cases, where specific site investigations are not performed. Since the recommended time histories can reasonably reflect the local seismic hazards at these cities, they should be used as

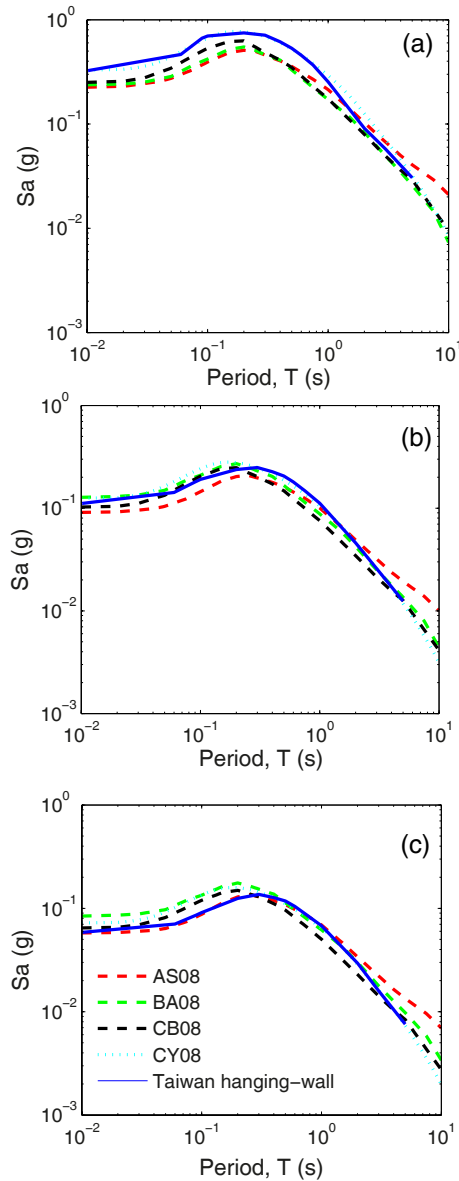


Figure 16. Comparison of spectral acceleration predicted using the local ground-motion prediction equation (GMPE) (Lin et al., 2011) and NGA global GMPEs under three earthquake scenarios: **(a)** $M = 7$, $R_{rup} = 10$ km, $V_{s30} = 760$ m s⁻¹; **(b)** $M = 7$, $R_{rup} = 30$ km, $V_{s30} = 760$ m s⁻¹; **(c)** $M = 7$, $R_{rup} = 50$ km, $V_{s30} = 760$ m s⁻¹.

basic results and then be serviceable for common engineering practice. The proposed ground-motion selection approach can also find applications in selecting appropriate time histories at bedrock layers, as input motions for a more comprehensive site investigation and seismic site response analysis.

Data availability. All data are available upon request from the corresponding author.

Competing interests. The authors declare that they have no conflict of interest.

Acknowledgements. The first author acknowledges financial support provided by Jockey Club Institute for Advanced Study at the Hong Kong University of Science and Technology for this work.

Edited by: Andreas Günther

Reviewed by: two anonymous referees

References

- Abrahamson, N. A. and Silva, W. J.: Summary of the Abrahamson & Silva NGA ground motion relations, *Earthq. Spectra*, 24, 67–97, 2008.
- Baker, J. W.: Conditional mean spectrum: Tool for ground-motion selection, *J. Struct. Eng.*, 137, 322–331, 2010.
- Baker, J. W. and Jayaram, N.: Correlation of spectral acceleration values from NGA ground motion models, *Earthq. Spectra*, 24, 299–317, 2008.
- Bommer, J. J.: Uncertainty about the uncertainty in seismic hazard analysis, *Eng. Geol.*, 70, 165–168, 2003.
- Bommer, J. J. and Acevedo, A. B.: The use of real earthquake accelerograms as input to dynamic analysis, *J. Earthq. Eng.*, 1, 43–91, 2004.
- Bommer, J. J., Scott, S. G., and Sarma, S. K.: Hazard-consistent earthquake scenarios, *Soil Dyn. Earthq. Eng.*, 19, 219–231, 2000.
- Boore, D. M. and Atkinson, G. M.: Ground-motion prediction equations for the average horizontal component of PGA, PGV, and 5 % damped PSA at spectral periods between 0.01 s and 10.0 s, *Earthq. Spectra*, 24, 99–138, 2008.
- Campbell, K. W.: Near-source attenuation of peak horizontal acceleration, *B. Seismol. Soc. Am.*, 71, 2039–2070, 1981.
- Campbell, K. W. and Bozorgnia, Y.: NGA ground motion model for the geometric mean horizontal component of PGA, PGV, PGD, and 5 % damped linear elastic response spectra for periods ranging from 0.01 s to 10.0 s, *Earthq. Spectra*, 24, 139–171, 2008.
- Castanos, H. and Lomnitz, C.: PSHA: is it science?, *Eng. Geol.*, 66, 315–317, 2002.
- CES, Central Geological Survey, <http://www.moeacgs.gov.tw/english2/index.jsp>, last access: 10 August 2017.
- Cheng, C. T.: Uncertainty analysis and de-aggregation of seismic hazard in Taiwan, PhD dissertation, Institute of Geophysics, National Central University, Chung-Li, Taiwan, 2002.
- Cheng, C. T., Chiou, S. J., Lee, C. T., and Tsai, Y. B.: Study on probabilistic seismic hazard maps of Taiwan after Chi-Chi earthquake, *Journal of GeoEngineering*, 2, 19–28, 2007.
- Chiou, B. S. J. and Youngs, R. R.: Chiou-Youngs NGA ground motion relations for the geometric mean horizontal component of peak and spectral ground motion parameters, *Earthq. Spectra*, 24, 173–215, 2008.
- Chiou, B. S. J., Darragh, R., Gregor, N., and Silva, W.: NGA project strong motion database, *Earthq. Spectra*, 24, 23–44, 2008.
- Du, W. and Wang, G.: A simple ground-motion prediction model for cumulative absolute velocity and model validation, *Earthquake Eng. Struc.*, 42, 8, 1189–1202, 2013.

- Du, W. and Wang, G.: Fully probabilistic seismic displacement analysis of spatially distributed slopes using spatially correlated vector intensity measures, *Earthquake. Eng. Struc.*, 43, 661–679, 2014.
- Foulser-Piggott, R. and Stafford, P. J.: A predictive model for Arias intensity at multiple sites and consideration of spatial correlations, *Earthquake. Eng. Struc.*, 41, 431–451, 2012.
- Gasparini, D. A. and Vanmarcke, E. H. E. J.: Simulated earthquake motions compatible with prescribed response spectra, Department of Civil Engineering, MIT, Cambridge, Mass, USA, 1976.
- Huang, D. and Wang, G.: Stochastic simulation of regionalized ground motions using wavelet packets and cokriging analysis, *Earthquake. Eng. Struc.*, 44, 775–794, <https://doi.org/10.1002/eqe.2487>, 2015a.
- Huang, D. and Wang, G.: Region-specific spatial cross-correlation model for regionalized stochastic simulation of ground-motion time histories, *B. Seismol. Soc. Am.*, 105, 272–284, <https://doi.org/10.1785/0120140198>, 2015b.
- Huang, D. and Wang, G.: Energy-compatible and spectrum-compatible (ECSC) ground motion simulation using wavelet packets, *Earthq. Eng. Struc.*, 46, 1855–1873, <https://doi.org/10.1002/eqe.2887>, 2017.
- Jayaram, N., Lin, T., and Baker, J. W.: A computationally efficient ground-motion selection algorithm for matching a target response spectrum mean and variance, *Earthq. Spectra*, 27, 797–815, 2011.
- Joshi, A., Mohan, K., and Patel, R. C.: A deterministic approach for preparation of seismic hazard maps in North East India, *Nat. Hazards*, 43, 129–146, 2007.
- Klugel, J. U.: Seismic hazard analysis – Quo vadis?, *Earth-Sci. Rev.*, 88, 1–32, 2008.
- Kolathayar, S. and Sitharam, T. G.: Comprehensive probabilistic seismic hazard analysis of the Andaman-Nicobar regions, *B. Seismol. Soc. Am.*, 102, 2063–2076, 2012.
- Krinitzsky, E. L.: How to obtain earthquake ground motions for engineering design, *Eng. Geol.*, 70, 157–163, 2003.
- Lin, P. S. and Lee, C. T.: Ground-motion attenuation relationships for subduction-zone earthquakes in northeastern Taiwan, *B. Seismol. Soc. Am.*, 98, 220–240, 2008.
- Lin, P. S., Lee, C. T., Cheng, C. T., and Sung, C. H.: Response spectral attenuation relations for shallow crustal earthquakes in Taiwan, *Eng. Geol.*, 121, 150–164, 2011.
- Luco, N. and Cornell, C. A.: Structure-specific scalar intensity measures for near-source and ordinary earthquake ground motions, *Earthq. Spectra*, 23, 357–392, 2007.
- Moratto, L., Orlecka-Sikora, B., Costa, G., Suhadolc, P., Papaioannou, C., and Papazachos, C. B.: A deterministic seismic hazard analysis for shallow earthquakes in Greece, *Tectonophysics*, 442, 66–82, 2007.
- Mualchin, L.: History of Modern Earthquake Hazard Mapping and Assessment in California Using a Deterministic or Scenario Approach, *Pure Appl. Geophys.*, 168, 383–407, 2011.
- Sitharam, T. G. and Vipin, K. S.: Evaluation of spatial variation of peak horizontal acceleration and spectral acceleration for south India: a probabilistic approach, *Nat. Hazards*, 59, 639–653, 2011.
- Sokolov, V., Loh, C. H., and Wen, K. L.: Empirical study of sediment-filled basin response: The case of Taipei city, *Earthq. Spectra*, 16, 681–787, 2000.
- Sokolov, V., Wen, K. L., Miksat, J., Wenzel, F., and Chen, C. T.: Analysis of Taipei basin response for earthquakes of various depths, *Terr. Atmos. Ocean Sci.*, 20, 687–702, 2009.
- Stirling, M., Litchfield, N., Gerstenberger, M., Clark, D., Bradley, B., Beavan, J., McVerry, G., Van, Dissen, R., Nicol, A., Wallace, L., and Buxton, R.: Preliminary probabilistic seismic hazard analysis of the CO2CRC Otway project site, Victoria, Australia, *B. Seismol. Soc. Am.*, 101, 2726–2736, 2011.
- Tsai, Y. B.: Seismotectonics of Taiwan, *Tectonophysics*, 125, 17–37, 1986.
- USNRC: A performance-based approach to define the site-specific earthquake ground motion, United States Nuclear Regulatory Commission, Washington, 2007.
- Wang, G.: A ground motion selection and modification method capturing response spectrum characteristics and variability of scenario earthquakes, *Soil Dyn. Earthq. Eng.*, 31, 611–625, 2011.
- Wang, G. and Du, W.: Empirical correlations between cumulative absolute velocity and spectral accelerations from NGA ground motion database, *Soil Dyn. Earthq. Eng.*, 43, 229–236, 2012.
- Wang, G. and Wei, J.: Microstructure evolution of granular soils in cyclic mobility and post-liquefaction process, *Granul. Matter*, 18, 51, <https://doi.org/10.1007/s10035-016-0621-5>, 2016.
- Wang, G., Youngs, R., Power, M., and Li, Z.: Design ground motion library: an interactive tool for selecting earthquake ground motions, *Earthq. Spectra*, 31, 617–635, 2015.
- Ye, J. H. and Wang, G.: Seismic dynamics of offshore breakwater on liquefiable seabed foundation, *Soil Dyn. Earthq. Eng.*, 76, 86–99, 2015.
- Ye, J. H. and Wang, G.: Numerical simulation of the seismic liquefaction mechanism in an offshore loosely deposited seabed, *B. Eng. Geol. Environ.*, 75, 1183–1197, 2016.
- Zhang, G. and Wang, L.: Integrated analysis of a coupled mechanism for the failure processes of pile-reinforced slopes, *Acta Geotechnica*, 11, 941–952, 2016.